Natural Product Sciences
20(4) : 262-268 (2014)

Inhibitory Effect of Rutaecarpine on Thioacetamide (TAA)-induced Hepatic Fibrosis

Hyunjin Ahn[1,†], Sung-Jin Lee[2,†], Kung-Woo Nam[3], and Woongchon Mar[1,*]

[1]*Natural Products Research Institute, College of Pharmacy, Seoul National University, Seoul 151-742, Republic of Korea*
[2]*Department of Animal Biotechnology, Kangwon National University, Chuncheon 200-701, Republic of Korea*
[3]*SCH Biomedical Human Resource Development Center, College of Natural Sciences, Soon Chun Hyang University, Asan 336-745, Republic of Korea*

Abstract – Rutaecarpine is one of the major alkaloids present in the fruits of *Evodia rutaecarpa*. In this study, rutaecarpine was evaluated, both *in vitro* and *in vivo*, for its hepatoprotective properties against thioacetamide (TAA)-induced hepatic fibrosis. The results showed that rutaecarpine inhibited TAA-induced cytotoxicity, reduced the expression of the fibrogenic cytokine transforming growth factor β1 (TGF-β1), and induced the expression of bcl-2. To evaluate its *in vivo* effects, animal models with TAA-induced hepatic fibrosis were utilized. Levels of liver tissue injury-associated enzymes, including alanine aminotransferase (ALT) and aspartate aminotransferase (AST) were monitored. TGF-β1 and the α-smooth muscle actin (α-SMA) were measured as markers of the protective effects on hepatic fibrosis. The AST and ALT levels in blood were greatly enhanced by TAA and completely blunted by rutaecarpine. Rutaecarpine led to the down-regulation of TGF-β and Bax mRNA expression, as well as the up-regulation of Bcl-2 and Bcl-X_L mRNA levels. In conclusion, rutaecarpine inhibited TAA-induced hepatic fibrosis and apoptosis by inducing the expression of Bcl-2 while blocking TGF-β1 in our TAA-intoxicated model.

Keywords – Rutaecarpine, *Evodia rutaecarpa*, Thioacetamide, Hepatic fibrosis

Introduction

The liver is an important organ in the maintenance of nitrogen homeostasis and its impairment results in a variety of nutritional derangements[1]. Chronic liver injury is caused by a variety of insults, including viral hepatitis, alcohol and drug abuse, and autoimmune hepatitis. Injury often spans months to years and results in liver fibrosis, leading eventually to cirrhosis and end-stage liver disease[2,3].

Hepatic fibrosis, a precursor of cirrhosis, is a consequence of severe liver damage. In the injured liver, extracellular matrix (ECM) components are produced in stellate cells (fat-storing cells, lipocytes) in the space of Disse, which function in intact liver lobules as the primary storage area for retinoids[4]. Hepatic fibrosis is a major histological finding associated with the progression of chronic liver disease to cirrhosis. It is characterized by the increased deposition of ECM components, in particular fibrillar collagens types I and III. Stellate cells are currently considered one of the major sources of ECM proteins in the liver; expansion of their pool is a key step in the fibrogenic process[5]. During the development of hepatic fibrosis, the stellate cell undergoes a process of activation and proliferation, transforming from a vitamin-A-storing quiescent cell into a myofibroblast-like cell, devoid of vitamin A. Activated stellate cells are characterized by overproduction of type-I collagen as well as other matrix proteins, cell enlargement with increased rough endoplasmic reticulum and by its expression of α-smooth muscle actin (α-SMA), which contributes to fibrosis[6-9]. A variety of cytokines can modulate the production of matrix proteins. Transforming growth factor β1 (TGF-β1) is one of the most important fibrogenic cytokines that regulate cell proliferation and differentiation within the liver[10].

Thioacetamide (TAA), a hepatotoxic reagent, previously used to induce liver cirrhosis, has been used to induce fibrosis in rats[9].

Rutaecarpine is a quinazolinocarboline alkaloid isolated from *Evodia rutaecarpa*, which has been used in

*Author for correspondence
Prof. Woongchon Mar, Natural Products Research Institute, College of Pharmacy, Seoul National University, San 56-1 Silim-dong, Gwanak-gu, Seoul 151-742, Korea
Tel: +82-2-880-2473; E-mail: mars@snu.ac.kr

†These authors contributed equally to this article

traditional Chinese medicine for the treatment of gastrointestinal disorders, headaches, and hypertension. This alkaloid has many pharmacological activities, including vasorelaxation, anti-thrombotic, anti-inflammatory and utero-tonic effects[11].

Our results indicate that daily administration of rutaecarpine reduces the activation of hepatic stellate cells and hepatocyte apoptosis associated with TAA-induced liver fibrosis development. Rutaecarpine effects were also associated with a significant reduction of TGF-β1.

Materials and methods

Materials – Calcium, magnesium-free HBSS (Hank's balanced salt solution), HBSS, collagenase, BSA, 3-[4, 5-dimethylthiazol-2-yl]-2,5-diphenyltetrazolium bromide (MTT), TAA, propidium iodide (PI), paraformaldehyde, hematoxylin and eosin (H&E) were purchased from Sigma (St. Louis, MO, USA). RNA extraction solution (Easy-Blue) and ONE-STEP RT-PCR PreMix Kit were purchased from Intron Biotechnology (Sungnam, Korea). The β-actin, TGF-β, Bax, Bcl-2, and Bcl-xL primer pairs were purchased from Bionics (Seoul, Korea). The immunodetection kit and biotinylated IgG were purchased from Vector Laboratories (Burlingame, CA, USA). The mouse monoclonal α-SMA and TGF-β antibody were purchased from Genetex (San Antonio, TX, USA). The TUNEL commercial kit was purchased from Chemicon (Bedford, MA, USA).

Cell isolation – Hepatocytes were isolated using the liver perfusion method with collagenase[12]. This procedure routinely yielded over 90% viability based on the trypan blue exclusion test. Male rats (> 250 g) were anesthetized with ether. The rats were perfused first with calcium, magnesium-free HBSS and then with calcium, magnesium, collagenase and proteinase containing HBSS buffer. The lobes were then minced and passed through a 100-μm filter to release the hepatocytes. The resultant cell suspension was washed twice with BSA containing HBSS buffer using centrifugation at 50 × *g* for 90 sec to separate the pellet. The supernatants were centrifuged at 50 × *g* for 5 min. After discarding the pellet, this step was repeated until no pellet formed. Centrifugation at 200 × *g* for 10 min formed a pellet that contained the stellate cells. Hepatocytes and stellate cells were resuspended in DMEM containing 10% FBS. The cells were incubated at 37 ºC (95% humidity, 5% CO_2).

Cell viability – Cell viability was assessed using the MTT assay[13]. Hepatocytes were cultured in 96-well plates and grown to confluence in DMEM containing 10% FBS under standard culture conditions for 5 days. The hepatocytes were then incubated with 50 mM TAA for 24 h. Thereafter, the cells were incubated for an additional 48 h in the presence of various concentrations of rutaecarpine. MTT was added for the last 4 h of the incubation. Reduction of MTT to formazan was assessed using an ELISA reader.

Fluorescence activated cell sorter analysis – Hepatocytes were collected after various treatments, centrifuged, resuspended in phosphate-buffered saline (PBS) at a density of 2.5×10^5 cells/mL, and incubated with 70% EtOH for at least 1 h at –20 ºC. Propidium iodide (PI; 50 mg/mL) was added and the cells were placed on ice until analysis[14]. Apoptosis was analyzed using an EPICS XL fluorescence-activated cell sorter (Beckman Coulter Inc., Miami, FL, USA).

Mouse hepatic fibrosis model – Specific pathogen-free male Balb/c mice (20 - 25 g body weight) were given an intraperitoneal (IP) injection of TAA (250 mg/kg body weight) three times per week for 2 weeks, and then administered daily for 3 weeks[12]. Rutaecarpine was given by IP injection for 4 weeks. Rutaecarpine treatment was administered during weeks 2, 3 and 4 of the TAA treatment. All animals were sacrificed after 4 weeks. Blood and liver samples were collected for further experiments. Serum samples and liver tissues for RNA preparation were frozen at –80 ºC until assayed. For histological analysis, liver tissues were fixed with 4% (w/v) neutral paraformaldehyde.

Serum analysis – Blood samples were collected and immediately centrifuged at 13000 rpm at 4 ºC, and the plasma was stored at –80 ºC until assayed. Serum aspartate aminotransferase (AST) and alanine aminotransferase (ALT) levels were measured using commercial kits and a chemistry analyzer (Hitachi, Tokyo, Japan).

Reverse transcriptase-PCR – Total RNA was extracted and transcribed into cDNA in 8 μL of reaction mixture using a One-Step RT-PCR PreMix Kit (Intron Biotechnology). RNA templates and gene-specific primers were added into the upper PCR tubes. The levels of expression of all transcripts were normalized against that of β-actin in the same tissue sample. The following thermal cycle was used: reverse transcription reaction at 45 ºC for 30 min, denaturation of RNA at 94 ºC for 5 min, followed by 30 cycles of 94 ºC for 1 min, 55 ºC for 1 min, and 72 ºC for 1 min, followed by a final extension step of 72 ºC for 7 min, conducted in a GeneAmp PCR system 2400 (Applied Biosystems, Foster, CA). PCR products were separated on a 1% agarose gel. After ethidium bromide staining, photographs were prepared using a LAS-1000 plus (Fuji, Tokyo, Japan).

Histochemistry – Liver specimens were immediately

removed and fixed in 4% neutral paraformaldehyde for 24 h, dehydrated in ethanol and embedded in paraffin. Tissue sections (5-μm thickness) were stained with H&E and observed under a light microscope[15].

Immunohistochemistry – Liver specimens were immediately removed and fixed in 4% neutral paraformaldehyde for 24 h, dehydrated in ethanol and embedded in paraffin. For immunohistochemistry, deparaffinized tissue sections, dehydrated in 100%, 95%, and 70% EtOH, were incubated with a primary antibody overnight in a humidified box and a secondary biotinylated IgG for 2 h in a humidified box, and staining was visualized using a Vector mouse-on-mouse immunodetection kit[16].

Terminal deoxynucleotidyl transferase-mediated dUDP nick end labeling staining – Terminal deoxynucleotidyl transferase-mediated dUDP nick end (TUNEL) was performed using a commercial kit. Liver specimens were immediately removed and fixed in 4% neutral paraformaldehyde for 24 h, dehydrated in ethanol and embedded in paraffin. For immunohistochemistry, deparaffinized tissue sections were dehydrated using 100%, 95%, and 70% EtOH. The non-specific chromogen reaction induced by endogenous peroxidase was inhibited with 3% H_2O_2 in MeOH for 10 min at room temperature. Terminal deoxynucleotidyl transferase (TdT) and the biotin-11-dUTP reaction were performed for 1 h at 37 °C in a humidified box, and a blocking reagent was applied for 30 min at room temperature, followed by avidin-horse radish peroxidase for 30 min at room temperature in a humidified box. Biochemical controls were made using positive-control slides treated with DNase, and negative-control slides treated with PBS instead of TdT. DNA fragments were stained using DAB as a substrate for the peroxidase, and methyl green was used as the counterstain[17].

Statistics – Data were subjected to ANOVA followed by Dunnett's multiple comparison method using GraphPad InStat 3 (GraphPad Software, San Diego, CA, USA).

Results

TAA-induced cytotoxicity in primary rat hepatocytes – To analyze the anti-apoptotic effects of rutaecarpine, apoptosis was induced in primary hepatocytes using TAA and cell viability was evaluated by MTT assay. Hepatocytes were exposed to 0.16, 0.8 or 4 μM rutaecarpine without TAA for 48 h. As shown in Fig. 1, Rutaecarpine showed 3.8%, 18.2% and 39.4% cytotoxicity at concentrations of 0.16, 0.8 and 4 μM, respectively. Hepatocytes in the presence of 50 mM TAA showed 84.3% cytotoxicity; however, the apoptotic ratios were 64.6%, 56.1%, and 31.1% in cells post-treated with 0, 0.16, 0.8 and 4 μM rutaecarpine, respectively.

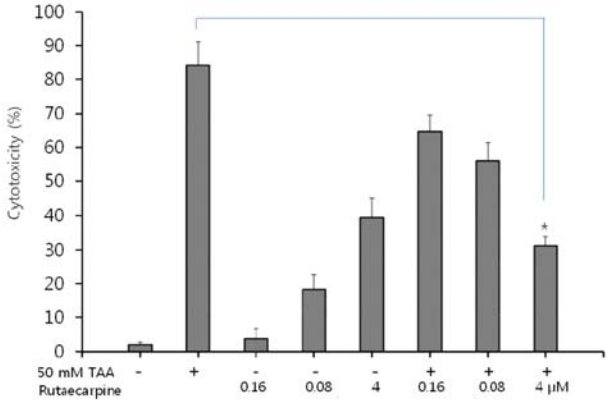

Fig. 1. Apoptosis of rutaecarpine-treated hepatocytes. Cells were treated with 0.16, 0.8 or 4 μM rutaecarpine for 48 h after 50 mM TAA for 24 h (*$p < 0.05$ *vs*. 50 mM TAA control).

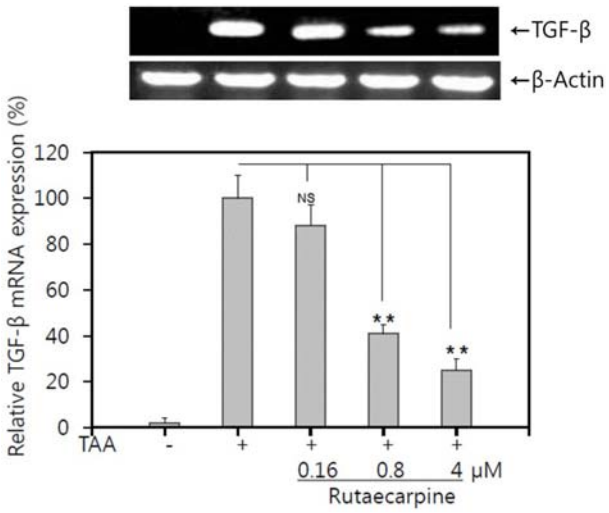

Fig. 2. RT-PCR analysis of TGF-β expression. RT-PCR was performed to determine the effect of rutaecarpine on TGF-β mRNA expression levels in primary cultured stellate cells. 1: vehicle control, 2: TAA (50 mM) alone, 3: TAA and rutaecarpine (0.16 μM), 4: TAA and rutaecarpine (0.8 μM) 5: TAA and rutaecarpine (4 μM) (**$p < 0.01$ *vs*. control; NS, not significant).

Rutaecarpine reduced the TGF-β expression – To explore the mechanism by which rutaecarpine reduces stellate cell activation, expression of TGF-β mRNA in the primary cultured stellate cells were detected by RT-PCR (Fig. 2). TAA increased TGF-β mRNA in the stellate cells 72 h after treatment, to a level approximately 10-fold higher than that of the vehicle control. In contrast, TGF-β mRNA levels were markedly decreased after treatment with rutaecarpine. Treatment with 4 μM rutaecarpine decreased relative TGF-β mRNA expression levels by 57.9%.

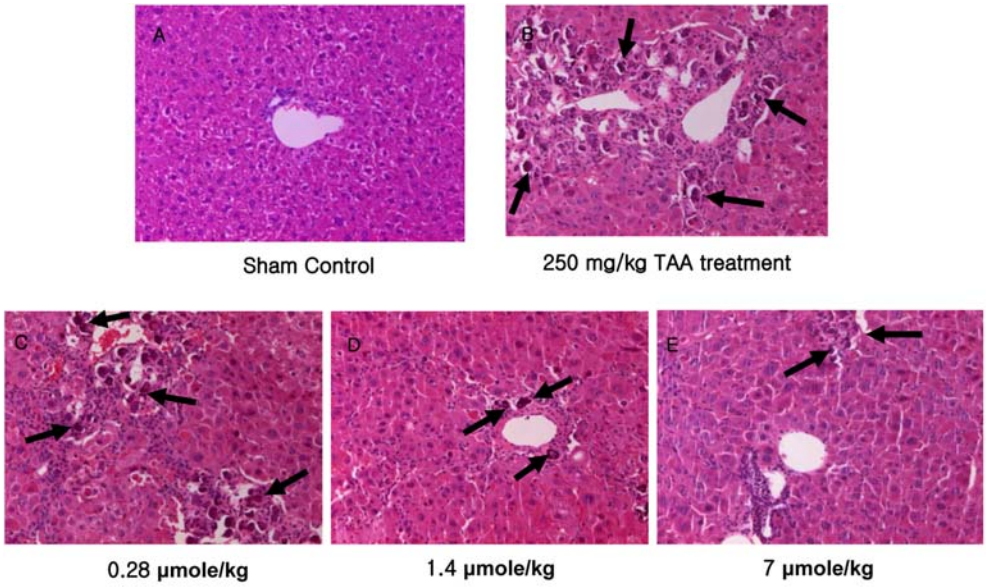

Fig. 3. Morphological analysis of liver treated with TAA (250 mg/kg) alone (B) or in combination with rutaecarpine (C, D, E); sham control (A). In this model, TAA administration induced continuous fibrotic septa (arrow). Livers were sectioned and hematoxylin-eosin–stained by standard techniques (magnification, × 200).

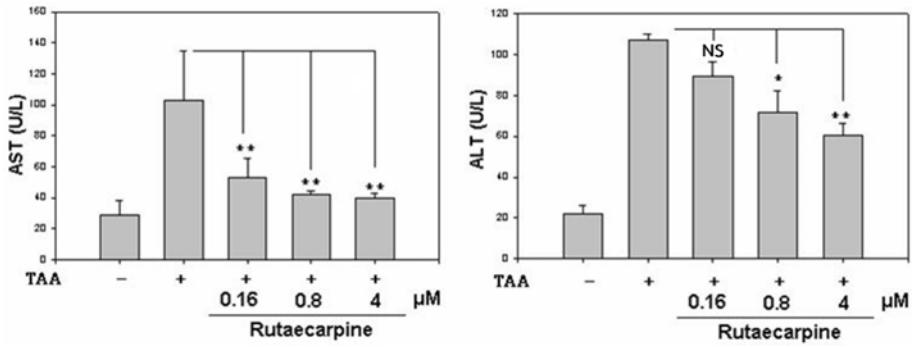

Fig. 4. The activities of the liver tissue injury-associated enzymes, (A) aspartate aminotransferase (AST) and (B) alanine aminotransferase (ALT), in blood were assayed. AST and ALT activities were markedly enhanced by TAA and blunted by rutaecarpine (*$p < 0.05$, **$p < 0.01$ *vs*. control; NS, not significant).

Histopathologic changes in mouse with TAA-induced liver fibrosis – Fig. 3 displays the microscopic appearance of TAA-induced fibrotic changes in the liver using H&E staining. The vehicle control exhibited no noticeable changes and showed a normal lobular architecture containing veins (Fig. 3A). Hepatocyte impairment, which was characterized by cell necrosis and nucleoli enlargement, was observed in the mouse liver treated with TAA for 5 weeks (Fig. 3B). In contrast, both necrotic and fibrotic changes were notably weaker when rutaecarpine was administered in conjunction with TAA (Fig. 3C, D, and E).

Effects on biochemical serum transaminases – Serum transaminases levels were measured to evaluate liver injury after TAA treatment. AST and ALT concentrations from control and TAA and rutaecarpine co-administration to mice are shown in Fig. 4. Blood AST and ALT concentrations were elevated after a single TAA injection. However, the concentrations were lower when rutaecarpine was administered together with TAA. During the experimental period, AST and ALT activities in mouse liver were greatly enhanced by TAA and completely blunted by rutaecarpine. Although still higher than those in the vehicle control, the administration of rutaecarpine (7 μmol/kg) decreased the serum AST and ALT levels by 62% and 44%, respectively.

Rutaecarpine regulates gene expressions in mice with TAA-induced liver fibrosis – TGF-β is an important fibrogenic cytokine that acts within the liver and has been implicated in the pathogenesis of hepatic fibrosis in

animals. We measured the expression of TGF-β mRNA in each specimen (Fig. 5). TGF-β mRNA levels relative to those of β-actin in the same sample were calculated.

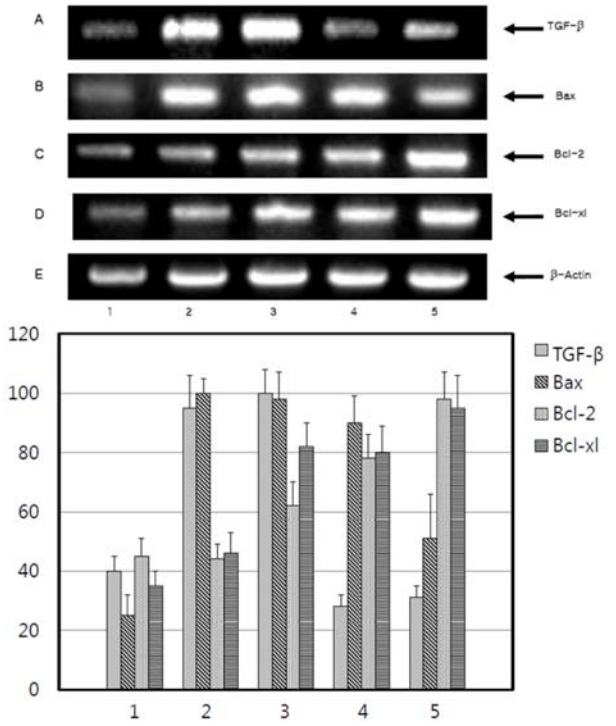

Fig. 5. RT-PCR analysis of a: TGF-β; b: Bax; c: Bcl-2; d: Bcl-xl; e: β-actin expression. RT-PCR was performed to determine the effect of rutaecarpine treatment on the levels of these genes mRNAs *in vivo*. 1: sham control, 2: TAA (250 mg/kg) alone, 3: TAA and rutaecarpine (0.28 μM), 4: TAA and rutaecarpine (1.4 μM) 5: TAA and rutaecarpine (7 μM).

RT-PCR analysis indicated that rutaecarpine decreased hepatic TGF-β mRNA levels by up to 62%. Therefore, rutaecarpine affected the regulation of TGF-β expression, which is consistent with its role in the inhibition of stellate cell activation.

Since the essential role of Bcl-2, Bcl-X_L and Bax is in the regulation of apoptosis, we examined the effects of rutaecarpine on the expression of these regulatory factors. RT-PCR analysis indicated that rutaecarpine decreased hepatic Bax mRNA levels by up to 2-fold, and increased those of Bcl-2 and Bcl- X_L by up to 50%. Thus, rutaecarpine had opposite effects on the regulation of Bcl-2, Bcl-X_L and Bax expression.

Immunohistochemical analysis of the expression of α-SMA and TGF-β – Activation of stellate cells is an essential process in the initiation and progression of hepatic fibrosis. Therefore, α-SMA and TGF-β expression in the liver, a specific marker of stellate cell activation, was assessed by immunohistochemistry. Liver sections showed positive staining for α-SMA (Fig. 6) and TGF-β (Fig. 7) 5 weeks after intraperitoneal administration of TAA and co-administration of rutaecarpine. The livers of mice treated with rutaecarpine after TAA administration (Fig. 6C, D and E) showed markedly reduced α-SMA expression. To clarify the underlying mechanisms by which activation of stellate cells is prevented in TAA-treated mice, hepatic TGF-β levels were evaluated using immunohistochemistry (Fig. 7). Hepatic TGF-β expression decreased after treatment with TAA and rutaecarpine (Fig. 7C, D and E).

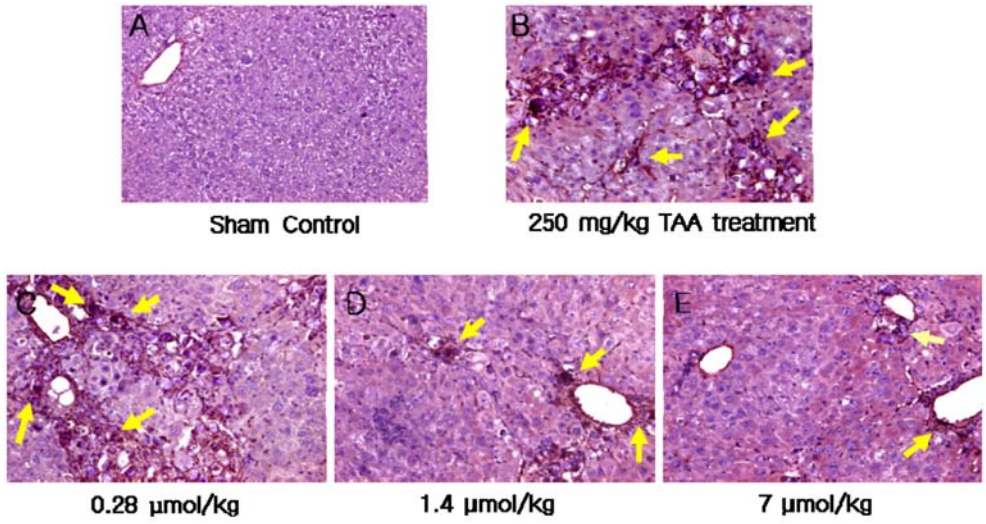

Fig. 6. Expression of α-SMA in the liver after administration of TAA. Control (A), TAA (250 mg/kg) alone (B), or in combination with rutaecarpine (C, D, E). Hepatic α-SMA expression after co-administration of TAA and/or rutaecarpine for 4 weeks was evaluated by immunohistochemical staining. α-SMA expression in centrilobular areas and periportal fibrotic bands in a TAA-treated mouse (arrow) (magnification, × 200).

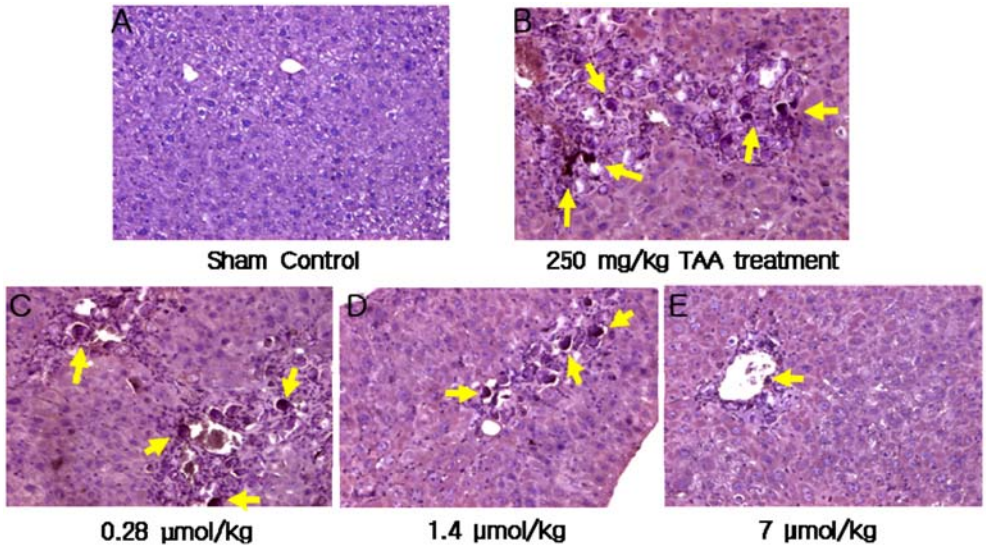

Fig. 7. Expression of TGF-β in the liver after administration of TAA. Control (A), TAA (250 mg/kg) alone (B), or in combination with rutaecarpine (C, D, E). Hepatic TGF-β expression after co-administration of TAA and/or rutaecarpine for 4 weeks was evaluated by immunohistochemical staining. TGF-β expression in areas of centrilobular and periportal fibrotic bands in TAA-treated mice (arrow) (magnification, × 200).

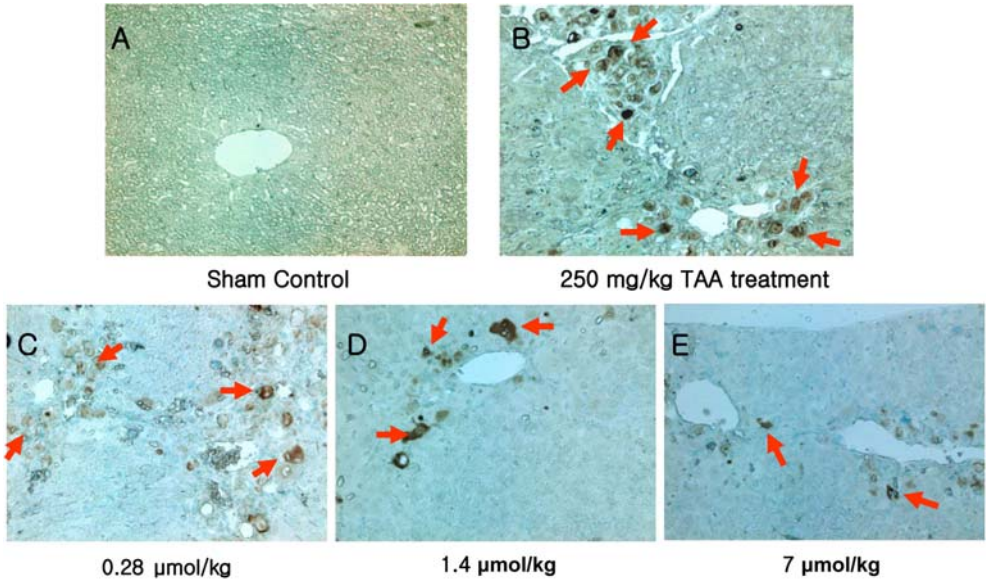

Fig. 8. DNA strand fragmentation demonstrated by the TUNEL technique (DAB staining with hematoxylin counterstaining of nuclei). Control (A), Mice were administrated TAA (250 mg/kg) alone (B), or in combination with rutaecarpine (C, D, E), as described previously. Positive (apoptosis) nuclei were stained brown (arrow) by the TUNEL reaction, and negative nuclei were stained blue (magnification, × 200).

Rutaecarpine reduced apoptosis in mice with TAA-induced liver fibrosis – Many chemical and physical treatments capable of inducing apoptosis are known to evoke oxidative stress. TAA administration induced DNA damage, nuclei shrinkage and condensation. As a result of TUNEL staining, the nuclei of apoptotic cells were stained brown and the TUNEL-positive cells consistently exhibited nuclear condensation. As TAA administration increased, more positive cells appeared; in contrast, addition of increasing amounts of rutaecarpine resulted in generation of fewer positive cells (Fig. 8).

Discussion

Liver cell injury or cell death is a common occurrence in many human conditions and illnesses. Therefore, an insight into the cellular mechanisms leading to cell death is relevant to understanding liver disease. Apoptosis is an

important mechanism of normal liver biology, and also a pathophysiological mechanism of cell death during hepatobiliary disease[18]. Many chemical and physical treatments capable of inducing apoptosis are known to evoke oxidative stress[19]. A variety of cytotoxic events can be produced by oxidative stress in hepatocytes when production of active oxidants overwhelms the antioxidant mechanisms. Treatment with rutaecarpine inhibited TAA-induced hepatotoxicity, as evidenced by PI staining.

In the normal liver, quiescent hepatic stellate cells are the precursor cells for myofibroblasts, which are responsible for the dramatic increase in extracellular matrix protein synthesis in the fibrotic liver[20]. Stellate cells when activated undergo a process in which they lose their vitamin A granules, proliferate, change morphologically into myofibroblasts, and then increase their synthesis of extracellular matrix proteins[21-22]. TGF-β is known as an important fibrogenic cytokine acting within the liver and acts to regulate cell proliferation, differentiation[23], and matrix synthesis[10]. Rutaecarpine may also modulate the effects of TGF-β (Fig. 2, 5), promoting stellate cell activation. These studies indicate that rutaecarpine is a potent inhibitor of both hepatocyte death and expression of TGF-β during the development of liver fibrosis.

In our study, chronic administration of TAA caused liver fibrosis and cirrhosis, as indicated by the changes in serum marker levels, and histopathological and molecular biological changes. TAA administration for 5 weeks led to fibrosis characterized by fibrous septa and severe alteration of hepatocyte structure (Fig. 3). The rutaecarpine-treatment group exhibited significantly decreased serum AST and ALT activities and TGF-β mRNA levels.

The major apoptotic signal transduction cascade associated with programmed cell-death converges into a common final pathway involving the Bcl-2-related protein family. Individual members of this group of proteins either promote cell survival (*e.g.*, Bcl-2 and Bcl-X_L) or induce cell death (*e.g.*, Bax, Bak and Bcl-X_s)[24], although Bcl-2 is thought to inhibit apoptosis by forming heterodimers with Bax. Bcl-2 in its homodimeric form also inhibits cell death by an alternate pathway[25].

In conclusion, rutaecarpine had significant anti-fibrosis effects on TAA-induced liver fibrosis in mice. The probable mechanisms include blocking of TGF-β expression, interfering with the activation of stellate cells, and or increasing the expression of survival genes, such as those of the Bcl family.

Acknowledgment

This work was supported by the Basic Science Research Program through the National Research Foundation of Korea (NRF) funded by the Ministry of Education, Science and Technology (Grant no. NRF-2013R1A1A 2008111) This work was also supported by BK21 Plus Program in 2014.

References

(1) Masumi, S.; Moriyama, M.; Kannan, Y.; Ohta, M.; Koshitani, O., Sawamoto, O.; Toyoshima, S.; Ishikawa, K.; Miyoshi, M.; Sugano, T. *Toxicology.* **1999**, *132*, 155-166.
(2) Han, E. K.; Park, C. I.; Lee, S. I. *Kor. J. Pathol.* **1990**, *24*, 412-422.
(3) Kurikawa, N.; Suga, M.; Kuroda, S.; Yamada, K.; Ishikawa, H. *Br. J. Pharmacol.* **2003**, *139*, 1085-1094.
(4) Shimizu, I.; Ma, Y. R.; Mizobuchi, Y.; Liu, F.; Miura, T.; Nakai, Y.; Yasuda, M.; Shiba, M.; Horie, T.; Amagaya, S.; Kawada, N.; Hori, H.; Ito, S. *Hepatology* **1999**, *29*, 149-160.
(5) Galli, A.; Svegliati-Baroni, G.; Ceni, E.; Milani, S.; Ridolfi, F.; Salzano, R.; Tarocchi, M.; Grappone, C.; Pellegrini, G.; Benedetti, A.; Surrenti, C.; Casini, A. *Hepatology* **2005**, *41*, 1074-1084.
(6) Fan, S.; Weng, C. F. *World J. Gastroenterol.* **2005**, *11*, 1411-1419.
(7) Rockey, D. C.; Housset, C. N.; Friedman, S. L. *J. Clin. Invest.* **1993**, *92*, 1795-1804.
(8) Tanaka, Y.; Nouchi, T.; Yamane, M.; Irie, T.; Miyakawa, H.; Sato, C.; Marumo, F. *J. Pathol*. **1991**, *164*, 273-278.
(9) Wu, J.; Norton, P. A. *Scand. J. Gastroenterol.* **1996**, *31*, 1137-1143.
(10) Border, W. A.; Noble, N. A. *N. Engl. J. Med.* **1994**, *331*, 1286-1292.
(11) Tsai, T. H.; Lee, T. F.; Chen, C. F.; Wang, L. C. *Pharmacol. Biochem. Behav.* **1995**, *50*, 293-298.
(12) Riccalton-Banks L.; Bhandari R.; Fry J.; Shakesheff K. M. *Mole. Cell. Biochem.* **2003**, *248*, 97-102.
(13) Kang, H. C.; Nan, J. X.; Park, P. H.; Kim, J. Y.; Lee, S. H.; Woo, S. W.; Zhao, Y. Z.; Park, E. J.; Sohn, D. H. *J. Pharm. Pharmacol.* **2002**, *54*, 119-126.
(14) Martindale, J. L.; Holbrook, N. J. *J. Cell Physiol.* **2002**, *192*, 1-15.
(15) Yang, X. J.; Liu, J.; Ye, L. B.; Yang, F.; Ye, L.; Gao, J. R.; Wu, Z. H. *World J. Gastroenterol.* **2006**, *12*, 1379-1385.
(16) Nan, J. X.; Park, E. J.; Kim, Y. C.; Ko, G.; Sohn, D. H. *J. Pharm. Pharmacol.* **2002**, *54*, 555-563.
(17) Imao, M.; Nagaki, M.; Imose, M.; Moriwaki, H. *Liver Int*. **2006**, *26*, 137-146.
(18) Patel, T.; Gores, G. J. *Hepatolgy* **1995**, *21*, 1725-1741.
(19) Buttke, T. M.; Sandstrom, P. A. *Immunol. Today* **1994**, *15*, 7-10.
(20) Friedman, S. L. *J. Biol. Chem.* **2000**, *275*, 2247-2250.
(21) Gressner, A. M. *Gut* **1994**, *35*, 1331-1333.
(22) Gressner, A. M.; Bachem, M. G. *Digestion* **1995**, *56*, 335-346.
(23) Grande, J. P. *Proc. Soc. Exp. Biol. Med.* **1997**, *214*, 27-40.
(24) Korsmeyer, S. J. *Trends Genet.* **1995**, *11*, 101-105.
(25) Zha, H.; Reed, J. C. *J. Biol. Chem.* **1997**, *272*, 31482-31488.

Received August 13, 2014
Revised September 10, 2014
Accepted September 10, 2014